Molecular Therapy
Methods & Clinical Development
Original Article

Highly efficient *in vivo* hematopoietic stem cell transduction using an optimized self-complementary adeno-associated virus

Carsten T. Charlesworth,[1] Shota Homma,[1,2] Anais K. Amaya,[3] Carla Dib,[1,3] Sriram Vaidyanathan,[7] Tze-Kai Tan,[1,5] Masashi Miyauchi,[1,2] Yusuke Nakauchi,[1,4] Fabian P. Suchy,[1,2] Sicong Wang,[1] Kyomi J. Igarashi,[1,2] M. Kyle Cromer,[6] Amanda M. Dudek,[1,3] Alvaro Amorin,[1,3] Agnieszka Czechowicz,[1,3] Adam C. Wilkinson,[8] and Hiromitsu Nakauchi[1,2,9]

[1]Institute for Stem Cell Biology and Regenerative Medicine, Stanford University School of Medicine, Lorry I. Lokey Stem Cell Research Building, 265 Campus Drive, Stanford, CA 94305, USA; [2]Department of Genetics, Stanford University School of Medicine, 279 Campus Drive, Stanford, CA 94305, USA; [3]Department of Pediatrics, Stanford University School of Medicine, 453 Quarry Road, Stanford, CA 94305, USA; [4]Department of Hematology, Stanford University School of Medicine, 269 Campus Drive, Stanford, CA 94305, USA; [5]Department of Pathology, Stanford University School of Medicine, 300 Pasteur Drive, Stanford, CA 94305, USA; [6]Department of Surgery, University of California, San Francisco, 400 Parnassus Ave, San Francisco, CA 94143, USA; [7]Center for Gene Therapy, Abigail Wexner Research Institute, Nationwide Children's Hospital, 700 Children's Drive, Columbus, OH 43215, USA; [8]Department of Haematology, Cambridge Stem Cell Institute, University of Cambridge, Puddicombe Way, Cambridge CB2 0AW, UK; [9]Stem Cell Therapy Laboratory, Institute of Integrated Research, Institute of Science Tokyo, 1-5-45 Yushima, Bunkyo-ku, Tokyo 113-8510, Japan

***In vivo* gene therapy targeting hematopoietic stem cells (HSCs) holds significant therapeutic potential for treating hematological diseases. This study uses adeno-associated virus serotype 6 (AAV6) vectors and Cre recombination to systematically optimize the parameters for effective *in vivo* HSC transduction. We evaluated various genetic architectures and delivery methods of AAV6, establishing an optimized protocol that achieved functional recombination in more than two-thirds of immunophenotypic HSCs. Our findings highlight that second-strand synthesis is a critical limiting factor for transgene expression in HSCs, leading to significant under-detection of HSC transduction with single-stranded AAV6 vectors. We also demonstrate that HSCs in the bone marrow (BM) are readily accessible to transduction, with neither localized injection nor mobilization of HSCs into the bloodstream, enhancing transduction efficacy. Additionally, we observed a surprising preference for HSC transduction over other BM cells, regardless of the AAV6 delivery route. Together, these findings not only underscore the potential of AAV vectors for *in vivo* HSC gene therapy but also lay a foundation that can inform the development of both *in vivo* AAV-based HSC gene therapies and potentially *in vivo* HSC gene therapies that employ alternative delivery modalities.**

INTRODUCTION

Hematopoietic stem cell (HSC) gene therapy is a groundbreaking and potentially life-saving form of treatment for genetic diseases of the hematopoietic system such as sickle cell disease, severe combined immunodeficiency, and Fanconi anemia.[1] This genetic form of therapy involves modifying or introducing nucleotide sequences into the genome of HSCs to cure disease. A wide array of technologies have been developed that allow for the genetic modification of an HSCs genome including lentiviral vectors, genome-modifying enzymes (such as base editors) and homology-directed repair (HDR)-based approaches, among others.[2–4]

These technologies have successfully been applied to HSCs *ex vivo* to cure genetic hematological diseases.[5–7] Although efficacious, the technical- and cost-intensive nature of these *ex vivo* HSC gene therapies has made their clinical implementation in patients a major challenge.[8] In contrast with *ex vivo* approaches, the development of *in vivo* gene therapies offers significant opportunities to improve patient accessibility to this form of therapy, due to the ability of *in vivo* gene therapy vectors to be mass manufactured and administered to patients via simple injection without the need for chemotherapy conditioning.

A wide variety of different delivery modalities have been developed to facilitate the delivery of genetic engineering enzymes, mRNA, and

Received 9 February 2024; accepted 18 February 2025;
https://doi.org/10.1016/j.omtm.2025.101438.

Correspondence: Agnieszka Czechowicz, Institute for Stem Cell Biology and Regenerative Medicine, Stanford University School of Medicine, Lorry I. Lokey Stem Cell Research Building, 265 Campus Drive, Stanford, CA 94305, USA.
E-mail:
Correspondence: Adam C. Wilkinson, Department of Haematology, Cambridge Stem Cell Institute, University of Cambridge, Puddicombe Way, Cambridge CB2 0AW, UK.
E-mail:
Correspondence: Hiromitsu Nakauchi, Department of Genetics, Stanford University School of Medicine, 450 Jane Stanford Way Stanford, CA 94305, USA.
E-mail: nakauchi@stanford.edu

DNA to cells *in vivo*.[9–12] Among the available platforms, adeno-associated virus (AAV) stands out as an attractive vector for *in vivo* HSC gene therapy due to its dual capability to express therapeutic transgenes and deliver DNA templates that can serve as donors for targeted integration approaches.[13,14] In addition, AAV vectors have also demonstrated efficacy as part of *ex vivo* HSC gene therapies and are capable of transducing HSCs *in vivo*.[15,16]

While a number of studies have demonstrated that HSCs can be transduced by gene therapy vectors *in vivo*, there is a paucity of studies that have systematically characterized and compared different methodologies for achieving transduction.[15,17–19] Here we sought to develop and characterize an optimized approach to achieve transduction of HSCs by AAV vectors *in vivo* and to systematically compare different approaches for achieving *in vivo* transduction of HSCs, focusing on the use of AAV6 due to its demonstrated efficacy for genetic engineering of human HSCs *ex vivo*.[16] Using the Ai14 (*Rosa26*$^{CAG\text{-}loxP\text{-}STOP\text{-}loxP\text{-}tdTomato}$) transgenic mouse model to detect HSC transduction of Cre-expressing AAVs via tdTomato (TdT) expression, we provide an AAV vector with an optimized genetic architecture for expression in HSCs and protocol for transduction of HSCs by AAV6 *in vivo*.

We demonstrate that (1) immunophenotypic HSCs can be transduced at rates of more than 80% *in vivo* by AAV6; (2) HSCs show a marked preference for AAV6 transduction compared with other bone marrow (BM) cells, which we hypothesize is due to their proximity to vascular niches, which potentially enhances their accessibility to vector transduction from the bloodstream; (3) HSCs are directly accessible to AAV6 transduction in the BM from the bloodstream, with neither localized injection nor mobilization significantly boosting transduction; (4) high doses of AAV6 are necessary for systemic delivery to HSCs, while lower doses mainly transduce the liver; and (5) second-strand synthesis is rate-limiting for transgene expression in HSCs, leading to significant underestimation of HSC transduction when using single-stranded AAV vectors.

Together these findings underscore the potential of AAV6 vectors for *in vivo* HSC gene therapy and highlight challenges to their clinical application. We anticipate that our findings can serve as a foundation for further development of *in vivo* AAV-based HSC gene therapies and potentially for therapies utilizing alternative delivery modalities, such as lipid nanoparticles (LNPs) or viral-like particles (VLPs).

RESULTS

AAV6 can transduce HSCs *in vivo*

To determine if we could transduce mouse HSCs *in vivo* we used AAV6 vectors that encoded a cytomegalovirus (CMV)-Cre-SV40 expression cassette and Ai14 mice. Successful transduction of cells and expression of Cre from AAV6 vectors can be detected in the Ai14 mouse model by the expression of TdT following Cre recombination (Figures 1A, 1B, and S1). Injecting AAV6 vectors at a dose of 1e11 or 1e12 vector genomes (vg) into Ai14 mice retro-orbitally (RO) we found that we could successfully transduce and induce Cre recombination in Lineage$^-$Sca1$^+$c-Kit$^+$ (LSK) hematopoietic stem and progenitor cells (HSPCs) at a dose of 1e12 vg (Figure 1C). Surprisingly, compared with other cell types in the BM HSPCs were preferentially transduced by AAV6 vectors ($p < 0.001$, ANOVA; $n = 5–6$).

An average of 16% of HSPCs were positive for TdT expression 3–4 weeks after injection compared with only 3% of the total population of cells in the BM (Figure 1C). Significantly lower rates of TdT$^+$ cells were found in the BM of mice transduced with 1e11 vg, with an average of only 0.1% of total BM cells positive for TdT expression and 1.1% of HSPCs (Figure 1C) ($p < 0.001$, ANOVA; $n = 5–6$). Analysis of peripheral blood (PB) from mice demonstrated that AAV6 vectors could also transduce PB cells when injected RO, albeit at lower frequencies than found in the BM (Figures 1D and S2). An average of 0.04% of CD45$^+$ cells were positive for expression of TdT at a dose of 1e11 vg and 0.1% at a dose of 1e12 vg. Recombination could be detected in both myeloid and lymphoid cells of the PB with 0.5% of myeloid cells (CD45$^+$CD11b/Gr1), 0.1% of B cells (CD45$^+$CD45R$^+$) and 0.06% of T-cells (CD45$^+$CD4/8$^+$) positive for TdT expression 3–4 weeks after injection of 1e12 vg of AAV6 (Figure 1D).

Off-target uptake by the liver has been a major challenge for achieving delivery to other desired cell types *in vivo* for a number of different gene therapy delivery modalities, including AAV vectors.[20] We hypothesized that high doses of AAV6 were required to transduce HSCs *in vivo* due to initial uptake of AAV6 by the liver, with significant systemic delivery to HSCs achieved only once the liver was saturated by AAV6 particles. Taking sections of livers and analyzing TdT expression, we found that at a dose of 1e11 vg an average of 45% of hepatocytes were TdT positive compared with 95% at a dose of 1e12 vg, in line with our hypothesis (Figures 1E and 1F) ($p < 0.01$, t test; $n = 5$).

Comparison of targeted HSC-specific delivery approaches

Having established that liver uptake was a rate-limiting factor for the delivery of AAV6 particles to HSCs, we next sought to divert the vectors from the liver to the BM (Figure 2A). We systematically investigated and compared localized injection routes and the mobilization of HSCs before RO injection, to standard venous injections of AAV6, to identify the most effective approach for maximizing *in vivo* transduction of HSCs. Prior work has demonstrated that injection into the caudal tail artery of mice can improve the engraftment of cells into the BM.[21] We, thus, first compared transduction of HSPCs when AAV6 was delivered by RO versus caudal artery injection. However, after injection of 1e12 vg of AAV6 into mice via the caudal artery or the RO vein, we found no statistically significant differences in the frequency of TdT$^+$ cells in the BM (Figure 2B) (ANOVA; $n = 6$).

We then compared direct injection of AAV6 into the BM by intrafemoral (IF) injection with RO injection. AAV6 vectors were injected into the left femur of mice at a dose of 1e12 vg and 3–4 weeks after injection the BM from the left and right femurs of mice was analyzed for TdT expression. Surprisingly, no statistically significant differences in the frequency of TdT$^+$ cells were found between injected

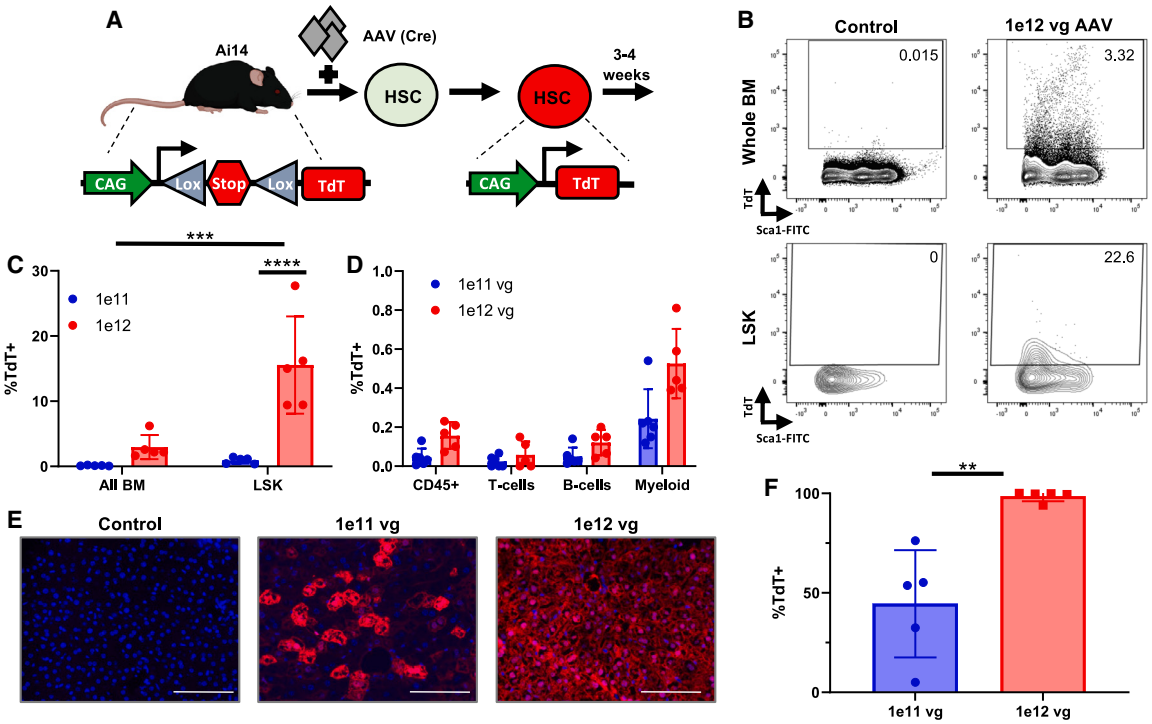

Figure 1. AAV6 preferentially transduces HSPCs in the BM at high doses

(A) Schematic outlining the experimental procedure for determining if AAV6 can transduce HSCs *in vivo* using Ai14 mice. (B) Representative FACS plots showing gating for TdT^+ positive cells in the general BM population and $Lin^-Sca1^+Kit^+$ HSPCs (LSK) after injection AAV6-Cre vectors into Ai14 mice. (C) Bar graph showing the frequency of TdT^+ cells in the BM of Ai14 mice after RO injection of AAV6 Cre at a dose of 1e11 vg or 1e12 vg (ANOVA, $n = 5$; mean ± SD). (D) Bar graph showing the frequency of TdT^+ PB cell types 3–4 weeks after RO injection of AAV6 Cre ($n = 5$; mean ± SD). (E) Representative images of liver sections taken from mice injected with AAV6-Cre compared with controls. DAPI-stained nuclei are shown in blue, cells expressing TdT are shown in red. Scale bar, 100 μm. (F) Bar graph showing the frequency of TdT^+ cells in the livers of mice injected with AAV6-Cre (t test; $n = 5$; mean ± SD). $^{**}p < 0.01$, $^{****}p < 0.0001$.

and non-injected femurs, or between IF and RO injection (Figure 2C) (ANOVA; $n = 6$). The lack of any significant differences between these conditions indicated that the BM is readily accessible to the bloodstream, with AAV6 immediately entering the bloodstream and traveling throughout the body systemically even after localized injection, leading to equivalent transduction frequencies in both femurs. It also indicated that we were potentially injecting saturating levels of AAV6 vectors into mice. Notably, regardless of the injection route utilized, a significantly higher fraction of HSPCs were transduced compared with other cell types in the BM (Figures 2B and 2C).

Prior work using adenovirus has found that mobilization of HSCs into the bloodstream can significantly improve transduction and we next sought to determine if this same approach was effective for AAV6.[18] HSCs were mobilized using a combination of granulocyte-colony stimulating factor (GCSF) and Plerixafor, after which AAV6 was injected into mice (Figure 2D). Flow cytometric analysis of PB samples collected directly before injection of AAV6 vectors confirmed that we were able to mobilize HSPCs in mice, with a significantly higher frequency of lineage negative and LSK cells found in the PB of mobilized mice compared with untreated controls (Figures 2E, 2G, and 2H) ($p < 0.05$, t test; $n = 3$–6). Analyzing TdT expression in cells 3–4 weeks after injection of 1e12 vg of AAV6, we found that mobilization actually led to a statistically significant decrease in transduction of both the general BM cell population and HSPCs (Figure 2F) ($p < 0.05$, t test; $n = 6$). No statistically significant differences were found in the frequency of LSK cells in the BM between the different routes and methods used to deliver AAV6 to mice, compared with untreated controls (Figure S3) (ANOVA; $n = 3$–6).

An optimized genetic architecture for detection of *in vivo* transduction

The studies described above used commercially available AAV6-Cre vectors that potentially did not have a genetic architecture optimal for transgene expression in HSPCs. Specifically, the vector expressed Cre via the CMV promoter, which has been reported to be silenced in hematopoietic cell types, and also uses the short viral SV40 polyA signal, which may not be optimal for RNA stability.[22,23] We hypothesized that this non-optimal genetic architecture may lead to significant under-representation of the percentage of HSPCs that were transduced by AAV6 vectors *in vivo* due to low levels of Cre expression in transduced cells.

We generated a series of GFP-expressing AAV6 vectors to compare promoter activity in HSPCs when different promoters (CMV, UBC,

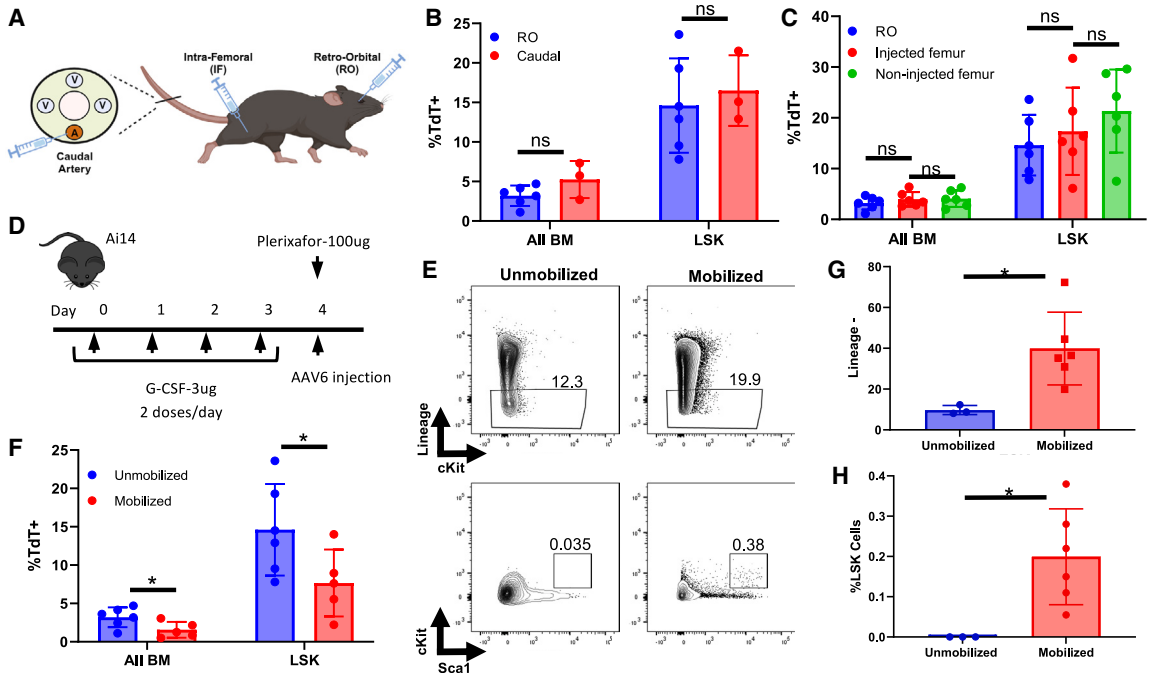

Figure 2. HSPCs are directly accessible to transduction in the BM

(A) Schematic showing the different locations where AAV6-Cre vectors were injected into mice. (B) Bar graph showing the frequency of recombination in the BM of mice injected with AAV6-Cre by RO compared with caudal artery injection (ANOVA; n = 3–6; mean ± SD). (C) Bar graph comparing the frequency of TdT$^+$ cells in the BM of mice injected with AAV6-Cre. RO delivery was compared with direct injection into the BM (femur) of mice, frequencies of TdT$^+$ cells in the BM were also compared between the injected femur and non-injected femur (ANOVA; n = 6; mean ± SD). (D) Schematic showing the procedure to mobilize HSCs before injection of AAV6-Cre vectors into mice. Black arrows indicate the days on which mice were injected with reagents. (E) Representative FACS plots of PB staining for lineage (top) and LSK HSPCs (bottom) after mobilization. (F) Bar graph comparing the frequency of TdT$^+$ cells in the BM of mice whose HSPCs were (mobilized) or were not (unmobilized) by treatment with GCSF and Plerixafor, before injection of AAV6-Cre vectors (ANOVA; n = 5–6; mean ± SD). (G) Bar graph comparing the frequency of Lin$^-$ cells in the PB of mice that were treated with GCSF and Plerixafor compared with mice that were not (t test; n = 3–6; mean ± SD). (H) Bar graph comparing the frequency of LSK cells in the PB of mice that were treated with GCSF and Plerixafor compared with mice that were not (t test; n = 3–6; mean ± SD). *p < 0.05, ns = not significant.

and SFFV) and polyA signal tails were used (SV40 and bGH polyA). Applying each vector to expanded C57BL/6J HSCs *in vitro* across a dose titration and analyzing for GFP expression 3 days later, we found that GFP expression could be detected at a surprisingly low frequency and intensity in cells regardless of the genetic architecture of the vector used (Figures 3A and 3B). An average of just 0.4% of HSCs could be detected as GFP positive at 3 days after transduction when a CMV-EGFP-SV40 AAV6 vector was applied to cells at a dose of 1e6 vg/cell (Figure 3D). Even with our most efficient vector (SFFV-GFP-bGH), we could only detect an average of 6% of HSCs as positive for GFP expression at a dose of 1e6 vg/cell (Figure 3D).

Our group and others have found that maximal delivery of a DNA donor to HSCs for *ex vivo* genetic engineering is achieved at doses of less than 1e4 vg/cell,[3,16] suggesting that a significantly greater fraction of HSCs is transduced by AAV6 both *in vitro* and *in vivo* than is detected by transgene expression. Second-strand synthesis is known to be a significantly rate-limiting step for AAV6 transgene expression in many tissues and we hypothesized that the low level of expression we detected was due to poor second-strand synthesis of AAV genomes in HSCs.[24]

Second-strand synthesis can be bypassed through the use of self-complementary AAV (scAAV) vectors (Figure 3C).[24] We, therefore, generated and compared GFP expression from single-stranded AAV6 (ssAAV6) vectors and scAAV6 vectors that had the same genetic architecture (SFFV-GFP-SV40) at a dose of 1e5 vg/cell (Figure 3E). We found that the use of an scAAV6 vector led to significantly greater GFP expression in HSCs. Using the scAAV6 vector, 95% of the HSCs became GFP$^+$, as compared with just 0.15% using the ssAAV6 vector (p < 0.05, t test; n = 3–6). We next generated ssAAV6 and scAAV6 vectors with the same genetic architecture to express Cre (SFFV-Cre-bGH) and applied these vectors to expanded Ai14 mouse HSCs. We found that scAAV6 vectors also induced significantly higher rates of recombination in this context (Figure 3F) (p < 0.0001 at 1e4 and 1e5 vg/cell doses, ANOVA; n = 7). By applying each vector to Ai14 HSCs across a dose titration and then analyzing TdT expression 1 week later, we found that at a dose of 1e4 vg/cell, 64% of HSCs were TdT$^+$ using scAAV, compared with just 11% for ssAAV.

Transduction of HSCs *in vivo* with scAAV6

Having detected significantly higher rates of recombination in HSCs when using our scAAV6 vector *in vitro*, we next applied this vector

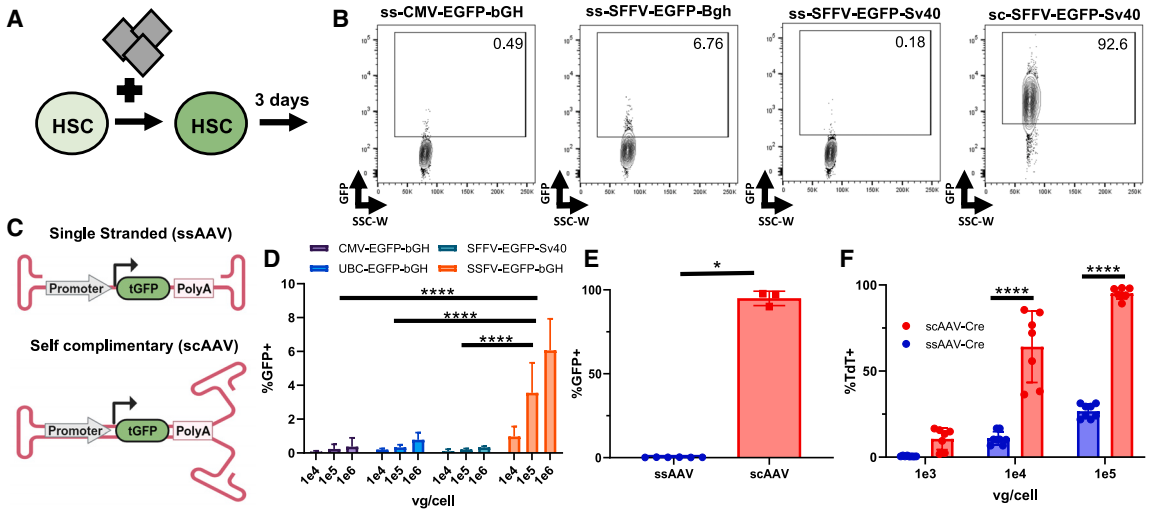

Figure 3. A genetically optimized AAV6 vector to detect transduction in HSCs

(A) Schematic outlining the procedure to compare the efficacy of different AAV6 constructs in expression of GFP, in expanded C57BL6/j HSCs *in vitro*. (B) Representative FACS plots from screening different AAV6 vectors for GFP expression in HSCs when AAV6 was added to cells at a dose of 1e5 vg/cell. (C) Schematic showing the design of different AAV6 cassettes to assess GFP expression and the difference in the genetic architecture of ssAAV vectors compared with scAAV vectors. (D) Bar graph showing the results from screening different ssAAV6 vectors on mouse HSCs *in vitro* for GFP expression (ANOVA; $n = 3$; mean ± SD). (E) Bar graph comparing the expression GFP from ssAAV and scAAV with the same optimized AAV6 genetic architecture (SFFV-GFP-SV40), 1e5 vg/cell of virus was used (t test; $n = 3$–6; mean ± SD). (F) Bar graph comparing the ability of optimized ssAAV and scAAV Cre expression vectors (SFFV-Cre-bGH) for their ability to induce recombination in Ai14 HSCs across a dose titration *in vitro* (ANOVA; $n = 7$; mean ± SD). $^{*}p < 0.05$, $^{****}p < 0.0001$.

in vivo to Ai14 mice. Injecting scAAV6 into mice at doses of 1e11 and 1e12 vg RO, we found significantly higher rates of AAV6 transduction and recombination *in vivo* when our optimized scAAV6 vectors were applied to Ai14 mice, compared with the original ssAAV6 vector we used (Figures 4A and 4B). Our scAAV6 vector led to not only significantly higher rates of recombination in the BM, but also in the LSK HSPC and $CD150^{+}CD48^{-}$LSK HSC populations at both doses tested ($p < 0.0001$, ANOVA; $n = 4$–5). Comparing each vector at a dose of 1e11 vg, we found that an average of 0.1% vs. 5.5% of total BM cells, 1.1% vs. 30% of LSK cells, and 0% vs. 36% of HSCs, were positive for TdT expression from ssAAV6 and scAAV6, respectively. At a higher dose of 1e12 vg, an average of 2.2% vs. 16.5% of BM cells, 16% vs. 62% of LSK cells, and 2.4% vs. 72% of HSCs were positive for TdT expression from ssAAV6 vs. scAAV6, respectively (Figure 4B). These results demonstrate that we could achieve significantly higher rates of AAV transduction within the immunophenotypic HSPC and HSCs populations' *in vivo* using scAAV6.

To assess the stability of the AAV genome in the BM of injected mice, we used digital droplet PCR to measure the relative frequency of AAV genomes compared with reference alleles from the mouse gene *Zeb2* in mice injected with 1e12 vg of AAV6. No significant difference was observed in the frequency of AAV genomes between mice injected with ssAAV and those injected with scAAV. Compared with the frequency of the mouse gene *Zeb2* an average of 0.5% ssAAV genomes were detected in the BM compared with 1.6% for scAAV 3–4 weeks after injection of AAV6 into mice (Figure S4A).

To further evaluate the stability of Cre vector expression in HSCs, we introduced Cre directly into the genome of mouse HSCs *in vitro* and tracked the persistence of Cre-expressing HSCs over time. Using the CRISPR-Cas9 system to create a double-stranded break at the *Rosa26* locus, we designed vectors to insert either a Cre-T2A-tGFP cassette or a fluorescent protein-only control cassette into the *Rosa26* locus via HDR, as previously described (Figures S4B–S4D).[16] Four days after editing, we observed successful integration and fluorescence in control samples with fluorescent protein-only cassettes; however, there was almost no detectable fluorescence in samples targeted with Cre-expressing cassettes (Figures S4B–S4D). Cre protein is known to have off-target activity and cause DNA damage, which HSCs are particularly sensitive to, suggesting that HSCs constitutively expressing Cre are negatively selected against.[25,26] Thus, the low persistence of AAV genomes in the BM compared with frequencies of TdT^{+} cells may be due to loss of the AAV genome during cell proliferation but may also be influenced by the cytotoxic effect of Cre expression in cells.

Higher rates of recombination were also found in the PB of mice treated with scAAV6 vectors as compared with ssAAV6 vectors, although to a lesser extent. An average of 0.1% and 0.6% of $CD45^{+}$ PB cells were positive for TdT expression from 1e12 vg of ssAAV6 vs. scAAV6, respectively (Figure 4C) ($p < 0.0001$, ANOVA; $n = 4$–5). Notably, a statistically significant decrease in the frequency of LSK cells was found in the BM of mice injected with 1e12 vg of scAAV6 as compared with ssAAV6 (Figure S3C) ($p < 0.05$, t test; $n = 4$–5). This may potentially be due to the increased immunogenicity of scAAV6 vectors and/or due to higher levels of Cre expression causing DNA

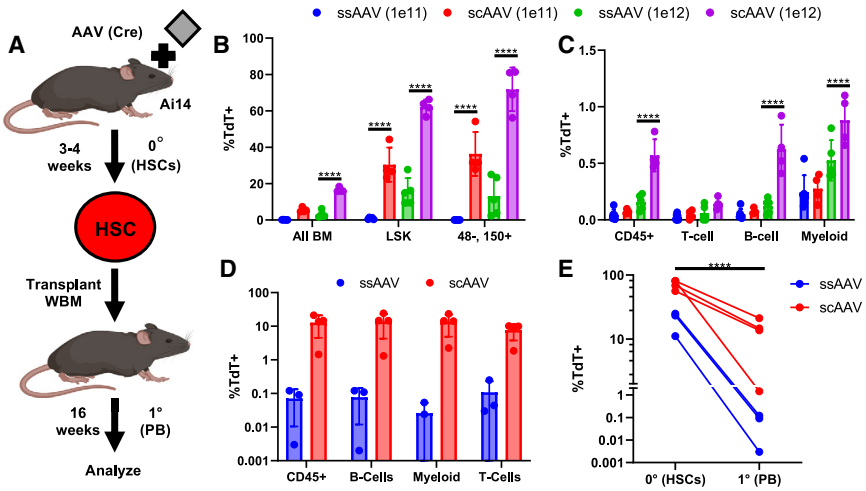

Figure 4. scAAV vectors demonstrate that significantly more HSPCs are transduced by AAV6 *in vivo* than is detected using ssAAV vectors

(A) Schematic outlining the experiments. Ai14 mice were injected with scAAV vectors and the ability of scAAV vectors to transduce cells was compared with ssAAV vectors 3–4 weeks after injection. To confirm that true HSCs were transduced by AAV6 WBM from injected mice was then transplanted into irradiated recipients and PB analyzed 16 weeks later. (B) Bar graph showing the frequency of TdT$^+$ cells in the BM of mice injected with either ssAAV-Cre or scAAV-Cre at a dose of 1e11 or 1e12 vg/mouse (ANOVA; n = 4–5; mean ± SD). (C) Bar graph showing the frequency of TdT$^+$ cells in the PB of mice injected with either ssAAV-Cre or scAAV-Cre at a dose of 1e11 or 1e12 vg/mouse (ANOVA; n = 4–5; mean ± SD). (D) Bar graph showing the frequency of TdT$^+$ cells in the PB of mice transplanted with BM from Ai14 mice injected with AAV-Cre at a dose of 1e12 vg, 16 weeks after transplantation (n = 3–4; mean ± SD). (E) Line graph comparing the frequency of LSK, CD48$^-$, CD150$^+$ TdT$^+$ cells in the BM of mice that received 1e12 vg of AAV (0°) to the frequency of CD45$^+$, TdT$^+$ cells in the PB of transplant recipients 16 weeks after transplantation (1°) (ANOVA; n = 3–4).***$p < 0.0001$.

damage in cells. No other statistically significant differences in the frequency of LSK cells (n = 4–5; t test) or PB cells (n = 4–5; ANOVA) were found between the two vectors or doses (Figures S3B–S3E).

To confirm that functional HSCs were successfully transduced by AAV6, whole BM (WBM) from mice injected with ssAAV6 or scAAV6 was then transplanted into lethally irradiated recipients. Analyzing the PB for TdT$^+$ cells at 16 weeks post-transplantation, we found TdT$^+$ cells from both conditions in both myeloid and lymphoid cells (Figures 4D and S3F). Notably, however, there was a significant drop in the frequency of TdT$^+$ cells in the PB of recipient mice as compared with the frequency of TdT$^+$ immunophenotypic HSCs in transduced mice (Figure 4E) ($p < 0.0001$, ANOVA; n = 3–4). For ssAAV6 transduced mice (at 1e12 vg, 0°), an average of 19.8% TdT$^+$ immunophenotypic HSCs in the BM 3–4 weeks after AAV6 injection led to an average of 0.5% of TdT$^+$CD45$^+$ cells in the transplant recipient PB (1°) 16 weeks after transplantation. For scAAV6 transduced mice (at 1e12 vg, 0°), an average of 72% TdT$^+$ immunophenotypic HSCs in the BM in the BM 3–4 weeks after AAV6 injection led to an average of 13% of CD45$^+$TdT$^+$ cells in the transplant recipient PB (1°) 16 weeks after transplantation.

This drop between injected mice and transplanted mice, could indicate that a lower frequency of functional HSCs are transduced compared with immunophenotypic HSCs, but may also potentially be due to AAV transduction or expression of Cre reducing the fitness of transduced cells. Despite these significant decreases, these data demonstrate that functionally transplantable HSCs are transduced in the BM of mice injected with AAV6 vectors.

Liver uptake is rate limiting for systemic delivery of AAV6 vectors *in vivo*

Finally, mice that were injected with scAAV6 vectors were imaged for TdT fluorescence to ascertain to what extent AAV6 vectors transduced tissues other than the hematopoietic system and liver. In mice that were injected with 1e11 vg of scAAV6, very high levels of TdT expression could be detected in the liver but only very low levels of fluorescence were detected in other tissues (Figures 5 and S5). By contrast, in mice injected with 1e12 vg scAAV6, high levels of TdT expression could be detected in the liver and in multiple other tissues of the body, including the intestines, ovaries, and skin (Figures 5 and S5). Comparing total body fluorescence between 1e11 and 1e12 conditions by imaging (after removal of the liver), we found that mice injected with 1e11 vg had a significantly lower level of total body fluorescence than mice injected with 1e12 vg ($p < 0.05$, t test; n = 4–5). Mice injected with 1e12 vg had 5-fold higher relative fluorescence units than 1e11 vg-injected mice, and over 30-fold higher than controls (Figure 5B).

Analysis of liver sections from mice injected with scAAV6 vectors revealed that 99% and 100% of hepatocytes were positive for TdT expression when 1e11 vg and 1e12 vg of scAAV6 were injected, respectively (Figure 5D). These results suggest that, even at the lower dose of AAV6 used, the liver was reaching saturating levels of transduction by AAV6, facilitating some level of systemic delivery of AAV6 vectors to HSCs. However, this was not detected when ssAAV6 vectors were injected into mice due to low levels of transgene expression.

DISCUSSION

Here we have demonstrated that AAV6 vectors can transduce functional HSCs *in vivo* at high efficiency and provide both an optimal protocol to transduce HSCs *in vivo*, including an scAAV6 vector with an optimal genetic architecture to detect transduction of HSCs. Our data highlight that HSCs are readily able to be transduced in the BM, a surprising preferential transduction of HSCs in the BM compared with other cell types, that second-strand synthesis is rate limiting for expression of a transgene from AAV6 vectors in HSCs

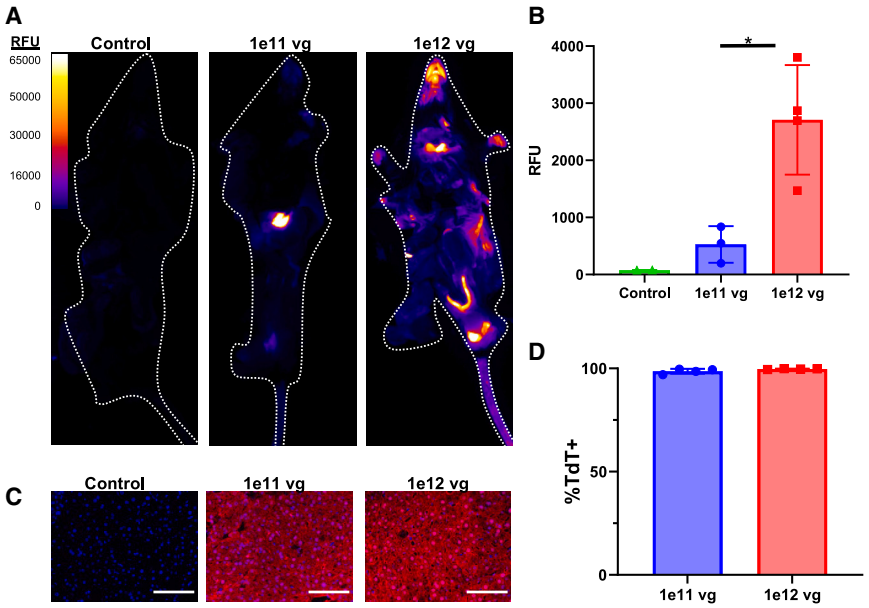

Figure 5. Saturation of the liver and systemic delivery to the body of AAV6 vectors at high doses

(A) Representative images of TdT fluorescence in Ai14 mice 3.5 weeks after injection with scAAV6 vectors. White dotted lines indicate the outline of mice in the image. (B) Bar graph comparing the difference in whole body fluorescence intensity of Ai14 mice injected with scAAV vectors at different doses compared with untreated control Ai14 mice (t test; $n = 2–4$; mean ± SD). (C) Representative images of liver sections from mice injected with scAAV6 vectors at different doses compared with control Ai14 mice. Blue indicates DAPI stained nuclei, red indicates cells expressing TdT. Scale bars, 100μm. (D) Bar graph showing the frequency of TdT^+ cells in the liver of mice treated with scAAV at a dose of 1e11 or 1e12 vg/mouse ($n = 4$; mean ± SD). *$p < 0.05$.

and highlight the challenge that off-target transduction by the liver poses to systemic delivery of AAV6 vectors to tissues throughout the body, including the BM.

Notably, the use of ssAAV6 vectors likely leads to underestimation of AAV6 transduction in many tissues due to low expression of transgenes, but poor episomal expression from AAV6 vectors seems to be particularly acute in HSCs. This under-representation is particularly important in the context of using AAV6 for delivery of transgenes or gene editing enzymes to HSCs, suggesting that AAV6 vectors are not ideal for either without further development to improve transgene expression. Notably, however, our scAAV6 data highlight that, even at moderate doses, AAV6 can transduce immunophenotypic HSCs at clinically relevant frequencies. Although our method of detection is indirect (tracking Cre recombination after expression of Cre from AAV vectors via TdT expression), our findings are in line with previous studies.[27]

Our results indicate that AAV6 vectors could readily prove to be a valuable vector for delivering DNA templates *in vivo* to HSCs, which can serve as a template for homology-directed repair (HDR) or homology-independent targeted integration. This approach could be especially effective if paired with a second delivery vector, such as LNPs, which can transiently deliver genetic engineering enzymes like CRISPR-Cas9, as has been demonstrated for the *in vivo* correction of hemophilia in the liver.[28,29]

Furthermore, we found that HSCs are preferentially transduced in the BM compared with other cell types, regardless of the delivery route. This consistent transduction efficiency suggests that HSCs are readily accessible to systemic delivery once liver uptake is overcome. Notably, our systematic comparison of different delivery routes indicates that, compared with simple venous injection, alternative localized delivery routes and HSC mobilization do not necessarily enhance HSC-specific transduction. We hypothesize that this trend is due to AAV vectors immediately going systemic after injection, regardless of the delivery route used, leading to equivalent levels of off-target liver transduction. However, this hypothesis would be further strengthened with a more in-depth analysis of AAV vector genomes in different organs, in particular the liver, after injection by different routes.

Additionally, the effective transduction of HSCs at high doses, once liver uptake is overcome, implies that while strategies such as conjugating anti-HSC antibodies or nanobodies to vectors may improve *in vivo* targeting, reducing off-target uptake by the liver is even more crucial for enhancing HSC targeting *in vivo*. High titers of virus were required (1e12 vg) to efficiently transduce HSCs, which present manufacturing challenges to clinical application. However, our data suggest that, if off-target liver transduction can be overcome, clinically relevant transduction of HSCs may be achieved by AAV6 vectors at clinically relevant doses that can be translated to patients.

The consistent preferential transduction of HSCs in the BM is a surprising finding of this study and our group has observed a similar trend when applying VLPs technology to target HSCs *in vivo* as well.[30] We hypothesize that HSC residence in vascular niches within the BM could be a cause for their preferential transduction in the BM by AAV6 vectors.[31] Close proximity to the bloodstream might facilitate better transduction of HSCs compared with other BM cell types that are situated farther from blood vessels. Preferential transduction of HSCs in the BM indicates that HSCs may make an ideal cell type for the development of *in vivo* gene therapies. However, other factors such as vector tropism could also be contributing to this preferential transduction, and further investigation is required to better characterize and explain this phenomenon.

A notable finding from this study was that significantly lower rates of recombination were detected in transplanted mice than observed in

the immunophenotypic HSCs of the transplanted BM. Furthermore, a low frequency of AAV genomes was detected in the BM of mice 3–4 weeks after injection. Transduction of HSCs by AAV6 vectors is known to cause differentiation and reduced engraftment of cells, and high levels of Cre expression are known to be toxic to cells due to DNA damage.[25,26] Notably, targeting HSCs at the *Rosa26* locus with a Cre-expressing cassette we found that Cre exerted strong negative selection pressure in HSCs. These effects may be contributing to the reduced fitness of the transduced HSCs in the transplant setting and may be exerting negative selection on transduced HSCs that stably express Cre as well. In line with this hypothesis, significantly lower frequencies of LSK cells were found in the BM of mice injected with scAAV6 vectors at a dose of 1e12 vg. Despite the significant drop upon transplantation, our data demonstrate that long-term functional HSCs are able to be transduced by AAV6 vectors at clinically relevant frequencies and are able to retain their self-renewal and multipotent differentiation capabilities in the long term after transduction.

In summary, this study underscores the potential of AAV6 vectors for *in vivo* HSC gene therapy while highlighting challenges and considerations for their effective application. Understanding the nuances of HSC transduction *in vivo*, including cellular barriers, tropism, optimal delivery methods and off-target effects, is crucial for advancing *in vivo* HSC gene therapies for the treatment of genetic hematopoietic diseases. We expect that many of the general principles we have found here that apply to AAV6 will also be applicable with other similar *in vivo* delivery modalities and hope that our findings can help to serve as a foundation for future studies.

MATERIALS AND METHODS

Data reporting

No statistical methods were used to predetermine the sample size. The experiments were not randomized, and the investigators were not blinded to outcome assessment.

HSC culture and transduction *in vitro*

HSCs from Ai14 mice were isolated, expanded, and cultured as previously described.[32,33] Briefly, mice were euthanized, femurs were collected from mice, and BM was flushed. BM was stained with anti-cKit (CD117) antibody (Miltenyi Biotech) conjugated to magnetic beads and HSCs were enriched by MACs (Miltenyi Biotech) following the manufacturer's instructions. Cells were then plated in HSC expansion media: F12 (Gibco), 0.1% PVA (Sigma Aldrich), 1% penicillin/streptomycin/glutamine (Gibco), 1% ITSX (Gibco), 100 ng/mL mTPO (PeproTech), and 10 ng/mL SCF (PeproTech), after which cells were cultured in hypoxic (5% O^2) conditions as previously described, resulting in a highly enriched and expanded population of mouse HSCs after 2–4 weeks.[32,33] For *in vitro* transduction experiments, 1e4 expanded HSCs were plated in 96-well CellBIND plates (costar) in 100 μL of expansion media and AAV6 vectors applied to HSCs at the specified titers. Media was changed once every 2–3 days after transduction and cells were analyzed for TdT expression 1 week after transduction by flow cytometry or 3 days after transduction for GFP using an LSR Fortessa flow cytometer (BD).

AAV6 vector production

In the case of ssAAV-CMV-Cre-SV40 poly constructs, vectors were produced, titered, and purchased from Virovek. In the case of scAAV-SFFV-Cre-Bgh PolyA constructs AAV6 vectors for all *in vivo* experiments and some *in vitro* experiments were produced, titered, and purchased from Vigene. In all other cases, AAV6 constructs were produced and titered as follows: Five 15-cm plates of 293T cells were prepared at a confluency of 80%, then transfected using 560 μg of PEI max, 110 μg of PDGM6 (Gift from the Porteus lab), and 30 μg of AAV expression vectors. At 48 h after transfection, cells were scraped from plates and pelleted, and AAV6 vectors purified from cell pellets using Takara AAVpro purification kits following the manufacturer's instructions. After purification, AAV6 vectors were titered using the ITR primer probes as described previously.[34] AAV6 expression constructs were cloned using HiFi DNA assembly following the manufacturer's instructions (NEB). The ssAAV backbone used was a gift from the Porteus lab; the scAAV backbone was obtained from Addgene (32396).

Injection of AAV6 vectors *in vivo*

All animal experiments were approved by the Adminstrative Panel on Laboratory Animal Care at Stanford University. Ai14 mice (007914) used throughout were either obtained directly from the Jackon Laboratory or were bred in house. RO, caudal artery, and IF injections were performed as previously described.[21,35] For experiments where HSCs were mobilized before transplantation mice were injected with 3.25 μg of GCSF twice daily subcutaneously, separated by 7- to 8-h intervals for 4 days. One hour before delivery of AAV6 vectors, 100 μg of Plerixafor was injected into mice intra-peritoneally. AAV6 vectors were then RO injected into mice 1 h after Plerixafor injection. Immediately before injection of AAV6 vectors PB was taken RO from mice and the frequency of LSK-positive cells in the PB was determined by staining with the lineage cocktail of antibodies described below for 30 min at 4°C. After 30 min cells were washed in PBS and then stained with the following cocktail of antibodies for 90 min at 4°C: CD34-fluorescein isothiocyanate (FITC) (RAM34; Invitrogen), cKit-APC (2B8; BioLegend), Sca1-PE (D7; BioLegend), APC Efluor 780-streptavidin (BioLegend), and BV421-CD45.2 (104; Invitrogen), after which cells were washed in PBS and re-suspended in PBS with propidium iodide (Sigma-Aldrich) at a concentration of 1 μg/μL after which cells were analyzed using an Aria flow cytometer (BD). All animal protocols were approved by the Administrative Panel on Laboratory Animal Care at Stanford University.

Analysis of Cre recombination *in vivo*

At 3–4 weeks after injection of AAV6, mice were analyzed and the level of recombination in cells determined based on TdT expression. For PB analysis mice were anesthetized and blood samples taken via retroorbital bleeds. Red blood cells were lysed using ammonium chloride solution (STEMCELL Technologies). PB was then stained for using the

following antibodies: FITC CD11b (M1/70; eBioscience), FITC-GR1/Ly-6G (1A8; BioLegend), APC-CD4 (RM4-5; Invitrogen), APC-CD8 (53–6.7; Invitrogen), APC Efluor 780-B220 (RA3-6B2; Invitrogen), and BV421-CD45.2 (104; Invitrogen). Cells were re-suspended in PBS (Corning) with propidium iodide (Sigma-Aldrich) at a concentration of 1 μg/mL; cells were then analyzed for TdT expression by flow cytometry. To analyze BM, mice were euthanized and femurs were collected from mice. Femurs were flushed after which lineage positive cells were stained for using the following cocktail combination of biotinylated antibodies (lineage cocktail) for 30 min at 4°C: Gr-1 (RB6-8C5; BioLegend), Ter-119 (TER-119; Invitrogen), CD4 (RM4-5; BioLegend), CD8 (54-6.7; BioLegend), B220 (RA3-6B2; BioLegend), and interleukin-7R (A7R34; BioLegend), after which cells were washed with PBS and then stained in the following cocktail for 30 min at 4°C: BV421-ckit (2B8; BioLegend), FITC-Sca1 (D7; BioLegend), and APC/Efluor780-streptavidin (BioLegend). In some cases, cells were also stained with CD48-FITC and CD150-APC. Cells were then re-suspended in PBS with propidium iodide at a concentration of 1 μg/mL and rates of recombination determined using an Aria flow cytometer (BD).

Droplet digital PCR for detecting AAV genome

BM samples were collected and stored in liquid nitrogen in Cryostor CS10 3–4 weeks after injection of AAV6 vectors into mice. Frozen cell pellets were thawed with 150 μL lysis buffer containing 0.1% SDS, 5 mM EDTA, 0.2 mg/mL proteinase K (Thermo Fisher Scientific), 15 mM tris (pH 7.8), and 100 mM NaCl. The cells pellets were mechanically disrupted by pipette trituration, heated to 55°C for 10 min, heated to 75°C for 10 min, and spun at 6,000×*g* for 1 min to remove debris.

Supernatant from the cell lysate was analyzed by droplet digital PCR (ddPCR) to compare the number of residual AAV genome copies (GCs) relative to mouse cells. To detect the ssAAV, a previously published primer/probe set was used to detect CRE.[36] Since the scAAV used an alternate version of CRE, a different primer/probe set was designed termed CREv2. For quantifying mouse cells, a previously published primer/probe set termed Zeb2 was used to count the number of mammalian cells.[36] All primers and probes were ordered from Integrated DNA Technologies. Probes contained a Zen-3′ Iowa Black quencher, and either a 5′ FAM or 5′ HEX fluorophore: CRE-Forward 5′-TTGGCAGAACGAAAACGCTG-3′, CRE-Reverse 5′-GGAAATCCATCGCTCGACCA-3′, CRE-Probe (FAM) 5′-CCGCAGGTGTAGAGAAGGCACT-3′, CREv2-Forward 5′-TTCGACCAGGTCAGATCCCT-3′, CREv2-Reverse 5′-CCCAGAAATGCGAGGTTCCT-3′, CREv2-Probe (FAM) 5′-CAGCGATCGGTGCCAGGACA-3′, Zeb2-Forward 5′-GGATGGGGAATGCAGCTCTT-3′, Zeb2-Reverse 5′-AGTGCGGCAGAATACAGCA-3′, Zeb2-Probe (HEX)-3′.

Each ddPCR reaction was prepared and analyzed with the QX200 ddPCR system (Bio-Rad) in accordance with Bio-Rad's standard recommendations for use with their ddPCR Supermix for Probes (No dUTP) unless otherwise stated. All reactions had a final volume of 20 μL, containing 2 μL cell lysate, 0.45 μM Zeb2-F primer, 0.45 μM Zeb2-R primer, 0.125 μM Zeb2 probe (HEX channel), and the same concentration of either CRE or CREv2 primers and probe (FAM channel). Thermocycler conditions: 95°C for 10 min; 50 cycles of 94°C for 30 s and 60°C for 60 s; 98°C for 10 min; and hold at 4°C.

ddPCR analysis and gating was performed using QX Manager Standard Edition Version 2.1.0.25 (Bio-Rad). After subtracting background (<0.5 copies/μL in all negative controls), CRE and CREv2 were divided by the number of Zeb2 copies/μL. The ratio was then multiplied by two (accounting for two copies of Zeb2 per cell) and reported as AAV GCs per cell.

Gene targeting of HSCs using AAV6

For experiments targeting HSCs at the *Rosa26* locus, cells were targeted as previously described.[3] In brief, HSCs were targeted using CRISPR-Cas9 RNP targeting the *Rosa26* locus, using the *Rosa26* sgRNA 5′-actccagtctttctagaaga-3′ and the 4D electroporation (Lonza) system utilizing program EO100. Cassettes for integration into the *Rosa26* locus were introduced using a previously described HDR cassette for the *Rosa26* locus.[3] AAV6 donors were added to cells immediately after electroporation at a concentration of 5,000 vg/cell. Media was changed the next day and cells were analyzed for integration of cassettes by FACS analysis as previously described.[16]

Cryosectioning

Livers were removed from mice after euthanasia and dissected into 5 × 5 mm pieces. Liver pieces were fixed in 4% paraformaldehyde and then placed in a 30% sucrose 70% PBS solution for 2–3 days, after which they were embedded in OCT (Sakura), snap frozen in liquid nitrogen, and stored at −80°C. Frozen sections of 5 μm were then made from livers using a Leica CM3050S Cryostat. After which sections were stained with DAPI for 5 min at a concentration of 1 μg/mL in PBS, after which sections were washed with PBS 2× for 5 min. After drying, tissue sections were covered with Immumount (Epredia) for coverslip. Sections were then analyzed for TdT and DAPI fluorescence using a Keyence BZ-X710 microscope with DAPI imaged on the DAPI filter (Keyence) and TdT expression on the TRITC filter (Keyence).

Whole mouse fluorescence analysis

To determine the frequency of recombination in tissues other than the liver and hematopoietic system, livers were removed from mice and TdT fluorescence measured using an ImageQuant 800 imager (Amersham). Whole mice were placed in the imager and fluorescence was analyzed using the Cy3 filter, 0.8 s exposure and 2 × 2 binning.

Image analysis

Brightness and contrast of liver sections was increased using PowerPoint. Whole mouse images were analyzed using FIJI, the relative fluorescence of mice was pseudo colored using the Fire look-up table. Brightness and contrast of whole mouse images was also adjusted using ImageJ and total body fluorescence determined using FIJI as well. DAPI-positive nuclei were counted using the

Analyze particles function with the size set to 700-infinity pixels and the circularity to 0–1. Frequencies of $TdT^{+/-}$ cells were counted manually by eye, four independent sections were taken per independent replicate and the average frequency of TdT^{+} cells between replicates used.

HSPC secondary transplantation and analysis

To functionally confirm Cre recombination in functional HSCs secondary transplants were performed as follows. We prepared 2e6 BM cells from primary mice injected with AAV6 vectors in 150 μL of PBS. Recipient Pepboy J mice (45.1, 002014) obtained from Jackson Laboratories were then lethally irradiated with a total of 9 Gy, separated into two doses of 4.5 Gy by 12-h intervals. After irradiation, mice were anesthetized with 2.5% isoflurane and 1e6 WBM cells were injected into recipient's RO. To analyze engraftment of cells into secondary recipients' PB was collected while mice were under anesthesia by RO bleed. Red blood cells were then lysed, stained, and analyzed as described above with the addition of BV421-CD45.1 antibody (A20, eBioscience) and the use of BUV395-CD45.2 antibody to the staining protocol (104; Invitrogen).

Statistical analysis

Two-way ANOVA tests and unpaired two-tailed t tests were performed as indicated in the figures, using Prism 9 software.

DATA AVAILABILITY

Data, further information, and requests for materials from this study are available through contacting the primary corresponding author (Dr. Hiromitsu Nakauchi; nakauchi@stanford.edu).

ACKNOWLEDGMENTS

C.T.C. is supported by the National Science Foundation Graduate Research Fellowship under Grant No. (DGE-1656518). H.N. was supported by the NIH (R01DK116944; R01HL147124), the Linux Foundation, the Stinehart-Reed Foundation, and the Japan Society for the Promotion of Science. A.C.W. was supported by the NIH (K99HL150218), the Leukemia and Lymphoma Society (3385-19), the Kay Kendall Leukaemia Fund, and the Royal Society (RG\R1\241347). A.K.A. is supported by the Elizabeth Nash Memorial Fellowship from CFRI and the Stanford Maternal and Child Health Research Institute Postdoctoral Support. This work was funded through grants from the NIH (R01DK116944 and R01HL147124).

AUTHOR CONTRIBUTIONS

C.T.C. conceptualized the research, performed experiments, analyzed data, and prepared the manuscript. S.H., S.V., M.K.C., M.M., C.D., Y.N., F.P.S., A.K.A., T.T., K.I., A.A. aided with experiments and edited the manuscript. S.W. and A.M.D. made significant conceptual contributions to the work. A.C., A.C.W., and H.N. supervised the research, helped conceptualize experiments and edited the manuscript.

DECLARATION OF INTERESTS

H.N. is a co-founder of and shareholder in Megakaryon, and Century Therapeutics. A.C.W. is a consultant for ImmuneBridge. A.C. discloses financial interests in the following entities working in the rare genetic disease space: Beam Therapeutics, Diantus Therapeutics, Editas Medicines, GV, Inograft Biotherapeutics, Jasper Therapeutics, Kyowa Kirin, Prime Medicine, Rocket Pharmaceuticals, STRM.Bio, Spotlight Therapeutics, and Teiko Bio. However, none of these companies had input into the design, execution, interpretation, or publication of the work in this manuscript.

DECLARATION OF GENERATIVE AI AND AI-ASSISTED TECHNOLOGIES IN THE WRITING PROCESS

During the preparation of this work the authors used ChatGPT for editing of the manuscript. After using this tool/service, the authors reviewed and edited the content as needed and take full responsibility for the content of the publication.

SUPPLEMENTAL INFORMATION

Supplemental information can be found online at https://doi.org/10.1016/j.omtm.2025.101438.

REFERENCES

1. Charlesworth, C.T., Hsu, I., Wilkinson, A.C., and Nakauchi, H. (2022). Immunological barriers to haematopoietic stem cell gene therapy. Nat. Rev. Immunol. *22*, 719–733. https://doi.org/10.1038/s41577-022-00698-0.

2. Aiuti, A., Roncarolo, M.G., and Naldini, L. (2017). Gene therapy for ADA-SCID, the first marketing approval of an ex vivo gene therapy in Europe: paving the road for the next generation of advanced therapy medicinal products. EMBO Mol. Med. *9*, 737–740. https://doi.org/10.15252/emmm.201707573.

3. Wilkinson, A.C., Dever, D.P., Baik, R., Camarena, J., Hsu, I., Charlesworth, C.T., Morita, C., Nakauchi, H., and Porteus, M.H. (2021). Cas9-AAV6 gene correction of beta-globin in autologous HSCs improves sickle cell disease erythropoiesis in mice. Nat. Commun. *12*, 686. https://doi.org/10.1038/s41467-021-20909-x.

4. Zeng, J., Wu, Y., Ren, C., Bonanno, J., Shen, A.H., Shea, D., Gehrke, J.M., Clement, K., Luk, K., Yao, Q., et al. (2020). Therapeutic base editing of human hematopoietic stem cells. Nat. Med. *26*, 535–541. https://doi.org/10.1038/s41591-020-0790-y.

5. Frangoul, H., Altshuler, D., Cappellini, M.D., Chen, Y.S., Domm, J., Eustace, B.K., Foell, J., de la Fuente, J., Grupp, S., Handgretinger, R., et al. (2021). CRISPR-Cas9 Gene Editing for Sickle Cell Disease and beta-Thalassemia. N. Engl. J. Med. *384*, 252–260. https://doi.org/10.1056/NEJMoa2031054.

6. Boztug, K., Schmidt, M., Schwarzer, A., Banerjee, P.P., Díez, I.A., Dewey, R.A., Böhm, M., Nowrouzi, A., Ball, C.R., Glimm, H., et al. (2010). Stem-cell gene therapy for the Wiskott-Aldrich syndrome. N. Engl. J. Med. *363*, 1918–1927. https://doi.org/10.1056/NEJMoa1003548.

7. Aiuti, A., Slavin, S., Aker, M., Ficara, F., Deola, S., Mortellaro, A., Morecki, S., Andolfi, G., Tabucchi, A., Carlucci, F., et al. (2002). Correction of ADA-SCID by stem cell gene therapy combined with nonmyeloablative conditioning. Science *296*, 2410–2413. https://doi.org/10.1126/science.1070104.

8. Dunleavy, K. (2021). With the Pricing Situation 'untenable' in Europe, Bluebird Will Wind Down its Operations in the 'broken' Market.

9. Rothgangl, T., Dennis, M.K., Lin, P.J.C., Oka, R., Witzigmann, D., Villiger, L., Qi, W., Hruzova, M., Kissling, L., Lenggenhager, D., et al. (2021). In vivo adenine base editing of PCSK9 in macaques reduces LDL cholesterol levels. Nat. Biotechnol. *39*, 949–957. https://doi.org/10.1038/s41587-021-00933-4.

10. Li, C., Wang, H., Georgakopoulou, A., Gil, S., Yannaki, E., and Lieber, A. (2021). In Vivo HSC Gene Therapy Using a Bi-modular HDAd5/35++ Vector Cures Sickle Cell Disease in a Mouse Model. Mol. Ther. *29*, 822–837. https://doi.org/10.1016/j.ymthe.2020.09.001.

11. Staahl, B.T., Benekareddy, M., Coulon-Bainier, C., Banfal, A.A., Floor, S.N., Sabo, J.K., Urnes, C., Munares, G.A., Ghosh, A., and Doudna, J.A. (2017). Efficient genome editing in the mouse brain by local delivery of engineered Cas9 ribonucleoprotein complexes. Nat. Biotechnol. *35*, 431–434. https://doi.org/10.1038/nbt.3806.

12. Ran, F.A., Cong, L., Yan, W.X., Scott, D.A., Gootenberg, J.S., Kriz, A.J., Zetsche, B., Shalem, O., Wu, X., Makarova, K.S., et al. (2015). In vivo genome editing using Staphylococcus aureus Cas9. Nature *520*, 186–191. https://doi.org/10.1038/nature14299.

13. Suzuki, K., Tsunekawa, Y., Hernandez-Benitez, R., Wu, J., Zhu, J., Kim, E.J., Hatanaka, F., Yamamoto, M., Araoka, T., Li, Z., et al. (2016). In vivo genome editing via CRISPR/Cas9 mediated homology-independent targeted integration. Nature *540*, 144–149. https://doi.org/10.1038/nature20565.

14. Wang, L., Yang, Y., Breton, C.A., White, J., Zhang, J., Che, Y., Saveliev, A., McMenamin, D., He, Z., Latshaw, C., et al. (2019). CRISPR/Cas9-mediated *in vivo*

gene targeting corrects hemostasis in newborn and adult factor IX-knockout mice. Blood *133*, 2745–2752. https://doi.org/10.1182/blood.2019000790.

15. Goldstein, J.M., Tabebordbar, M., Zhu, K., Wang, L.D., Messemer, K.A., Peacker, B., Ashrafi Kakhki, S., Gonzalez-Celeiro, M., Shwartz, Y., Cheng, J.K.W., et al. (2019). In Situ Modification of Tissue Stem and Progenitor Cell Genomes. Cell Rep. *27*, 1254–1264.e7. https://doi.org/10.1016/j.celrep.2019.03.105.

16. Dever, D.P., Bak, R.O., Reinisch, A., Camarena, J., Washington, G., Nicolas, C.E., Pavel-Dinu, M., Saxena, N., Wilkens, A.B., Mantri, S., et al. (2016). CRISPR/Cas9 β-globin gene targeting in human haematopoietic stem cells. Nature *539*, 384–389. https://doi.org/10.1038/nature20134.

17. Shi, D., Toyonaga, S., and Anderson, D.G. (2023). In Vivo RNA Delivery to Hematopoietic Stem and Progenitor Cells via Targeted Lipid Nanoparticles. Nano Lett. *23*, 2938–2944. https://doi.org/10.1021/acs.nanolett.3c00304.

18. Richter, M., Saydaminova, K., Yumul, R., Krishnan, R., Liu, J., Nagy, E.E., Singh, M., Izsvák, Z., Cattaneo, R., Uckert, W., et al. (2016). In vivo transduction of primitive mobilized hematopoietic stem cells after intravenous injection of integrating adenovirus vectors. Blood *128*, 2206–2217. https://doi.org/10.1182/blood-2016-04-711580.

19. Breda, L., Papp, T.E., Triebwasser, M.P., Yadegari, A., Fedorky, M.T., Tanaka, N., Abdulmalik, O., Pavani, G., Wang, Y., Grupp, S.A., et al. (2023). In vivo hematopoietic stem cell modification by mRNA delivery. Science *381*, 436–443. https://doi.org/10.1126/science.ade6967.

20. Raguram, A., Banskota, S., and Liu, D.R. (2022). Therapeutic *in vivo* delivery of gene editing agents. Cell *185*, 2806–2827. https://doi.org/10.1016/j.cell.2022.03.045.

21. Kuchimaru, T., Kataoka, N., Nakagawa, K., Isozaki, T., Miyabara, H., Minegishi, M., Kadonosono, T., and Kizaka-Kondoh, S. (2018). A reliable murine model of bone metastasis by injecting cancer cells through caudal arteries. Nat. Commun. *9*, 2981. https://doi.org/10.1038/s41467-018-05366-3.

22. Ngai, S.C., Rosli, R., Al Abbar, A., and Abdullah, S. (2015). DNA methylation and histone modifications are the molecular lock in lentivirally transduced hematopoietic progenitor cells. BioMed Res. Int. *2015*, 346134. https://doi.org/10.1155/2015/346134.

23. Salmon, P., Kindler, V., Ducrey, O., Chapuis, B., Zubler, R.H., and Trono, D. (2000). High-level transgene expression in human hematopoietic progenitors and differentiated blood lineages after transduction with improved lentiviral vectors. Blood *96*, 3392–3398.

24. McCarty, D.M. (2008). Self-complementary AAV vectors; advances and applications. Mol. Ther. *16*, 1648–1656. https://doi.org/10.1038/mt.2008.171.

25. Piras, F., and Kajaste-Rudnitski, A. (2021). Antiviral immunity and nucleic acid sensing in haematopoietic stem cell gene engineering. Gene Ther. *28*, 16–28. https://doi.org/10.1038/s41434-020-0175-3.

26. Loonstra, A., Vooijs, M., Beverloo, H.B., Allak, B.A., van Drunen, E., Kanaar, R., Berns, A., and Jonkers, J. (2001). Growth inhibition and DNA damage induced by Cre recombinase in mammalian cells. Proc. Natl. Acad. Sci. USA *98*, 9209–9214. https://doi.org/10.1073/pnas.161269798.

27. Wang, J., Xie, J., Lu, H., Chen, L., Hauck, B., Samulski, R.J., and Xiao, W. (2007). Existence of transient functional double-stranded DNA intermediates during recombinant AAV transduction. Proc. Natl. Acad. Sci. USA *104*, 13104–13109. https://doi.org/10.1073/pnas.0702778104.

28. Gillmore, J.D., Gane, E., Taubel, J., Kao, J., Fontana, M., Maitland, M.L., Seitzer, J., O'Connell, D., Walsh, K.R., Wood, K., et al. (2021). CRISPR-Cas9 In Vivo Gene Editing for Transthyretin Amyloidosis. N. Engl. J. Med. *385*, 493–502. https://doi.org/10.1056/NEJMoa2107454.

29. Han, J.P., Lee, Y., Lee, J.H., Chung, H.Y., Lee, G.S., Nam, Y.R., Choi, M., Moon, K.S., Lee, H., Lee, H., and Yeom, S.C. (2023). In vivo genome editing using 244-cis LNPs and low-dose AAV achieves therapeutic threshold in hemophilia A mice. Mol. Ther. Nucleic Acids *34*, 102050. https://doi.org/10.1016/j.omtn.2023.102050.

30. Charlesworth, C.T., Homma, S., Suchy, F., Wang, S., Bhadhury, J., Amaya, A.K., Camarena, J., Zhang, J., Tan, T.K., Igarishi, K., and Nakauchi, H. (2024). Secreted Particle Information Transfer (SPIT) - A Cellular Platform for In Vivo Genetic Engineering. Preprint at bioRxiv. https://doi.org/10.1101/2024.01.11.575257.

31. Chen, J.Y., Miyanishi, M., Wang, S.K., Yamazaki, S., Sinha, R., Kao, K.S., Seita, J., Sahoo, D., Nakauchi, H., and Weissman, I.L. (2016). Hoxb5 marks long-term haematopoietic stem cells and reveals a homogenous perivascular niche. Nature *530*, 223–227. https://doi.org/10.1038/nature16943.

32. Igarashi, K.J., Kucinski, I., Chan, Y.Y., Tan, T.K., Khoo, H.M., Kealy, D., Bhadury, J., Hsu, I., Ho, P.Y., Niizuma, K., et al. (2023). Physioxia improves the selectivity of hematopoietic stem cell expansion cultures. Blood Adv. *7*, 3366–3377. https://doi.org/10.1182/bloodadvances.2023009668.

33. Wilkinson, A.C., Ishida, R., Kikuchi, M., Sudo, K., Morita, M., Crisostomo, R.V., Yamamoto, R., Loh, K.M., Nakamura, Y., Watanabe, M., et al. (2019). Long-term ex vivo haematopoietic-stem-cell expansion allows nonconditioned transplantation. Nature *571*, 117–121. https://doi.org/10.1038/s41586-019-1244-x.

34. Aurnhammer, C., Haase, M., Muether, N., Hausl, M., Rauschhuber, C., Huber, I., Nitschko, H., Busch, U., Sing, A., Ehrhardt, A., and Baiker, A. (2012). Universal real-time PCR for the detection and quantification of adeno-associated virus serotype 2-derived inverted terminal repeat sequences. Hum. Gene Ther. Methods *23*, 18–28. https://doi.org/10.1089/hgtb.2011.034.

35. Nakauchi, Y., Ediriwickrema, A., Martinez-Krams, D., Zhao, F., Rangavajhula, A., Karigane, D., and Majeti, R. (2023). Simplified Intrafemoral Injections Using Live Mice Allow for Continuous Bone Marrow Analysis. J. Vis. Exp. https://doi.org/10.3791/65874.

36. Suchy, F.P., Karigane, D., Nakauchi, Y., Higuchi, M., Zhang, J., Pekrun, K., Hsu, I., Fan, A.C., Nishimura, T., Charlesworth, C.T., et al. (2025). Genome engineering with Cas9 and AAV repair templates generates frequent concatemeric insertions of viral vectors. Nat. Biotechnol. *43*, 204–213. https://doi.org/10.1038/s41587-024-02171-w.